Electronic Supplementary Information

Dyes embedded YAG:Ce^{3+}@SiO_2 composite phosphors toward warm wLEDs through radiative energy transfer: Preparation, characterization and luminescence properties

Guo-Hui Pan[a*], Huajun Wu[a], Shuai He[a,b], Liangliang Zhang[a], Zhendong Hao[a], Xia Zhang[a], Jiahua Zhang[a*]

[a]*State Key Laboratory of Luminescence and Applications, Changchun Institute of Optics, Fine Mechanics and Physics, Chinese Academy of Sciences, 3888 Dong Nanhu Road, Changchun 130033, China.*

[b]*University of Chinese Academy of Sciences, Beijing 100049, China*

To whom correspondence should be addressed: guohui.pan@aliyun.com, jhzhang@ciomp.ac.cn

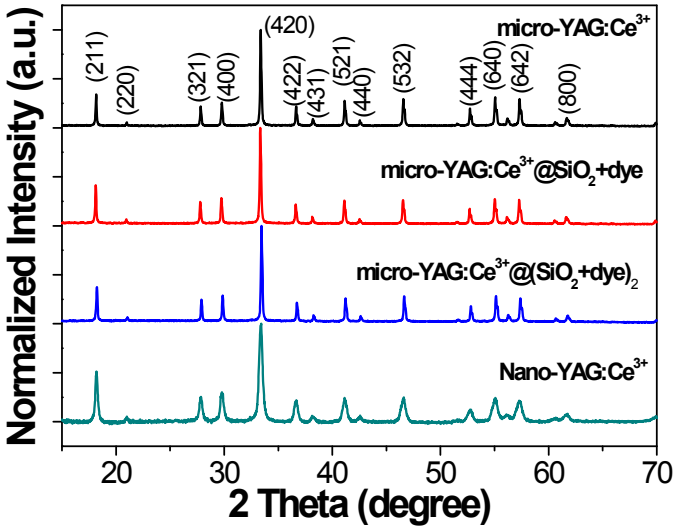

Fig. S1 XRD patterns of micro-YAG:Ce^{3+}, nano-YAG:Ce^{3+}, micro-YAG:Ce^{3+}@SiO_2+dye and micro-YAG:Ce^{3+}@(SiO_2+dye)$_2$.

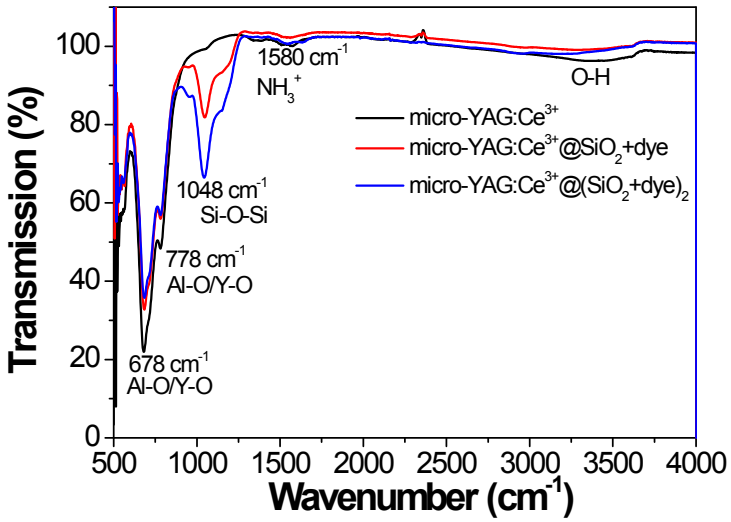

Fig. S2 FTIR spectra of micro-YAG:Ce^{3+}, micro-YAG:Ce^{3+}@SiO_2+dye and micro-YAG:Ce^{3+}@(SiO_2+dye)$_2$.

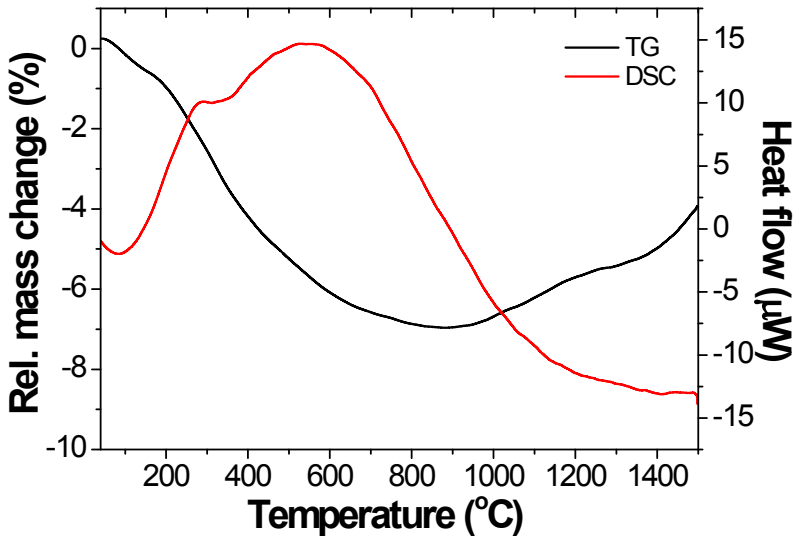

Fig. S3 TG-DSC curve of micro-YAG:Ce^{3+} in the range of 30-1500 °C.

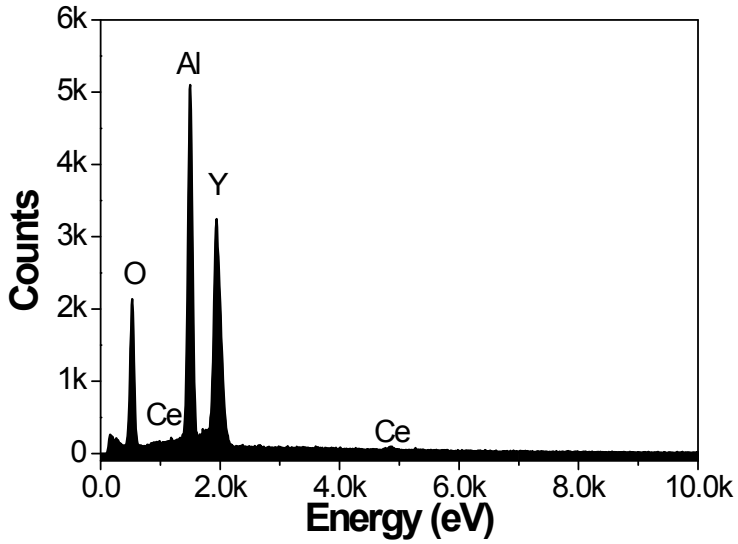

Elemental Analysis

Element	Weight %	Atomic %
O	29.57	56.92
Al	23.85	27.22
Y	44.39	15.38
Ce	2.18	0.48
Total	100	100

The Y(Ce) : Al Atomic raito is 15.86 : 27.22 = 0.58

Fig. S4 SEM-EDS spectra of micro-YAG:Ce^{3+} and the derived elemental analysis.

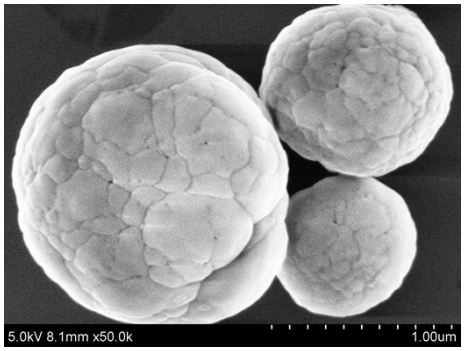

Fig. S5 SEM image of micro-YAG:Ce^{3+} after post-heat treatment at 1100 ^{o}C for 3 h in a quartz tube furnace under a flowing reducing gas (N_2/H_2, 95%/5%).

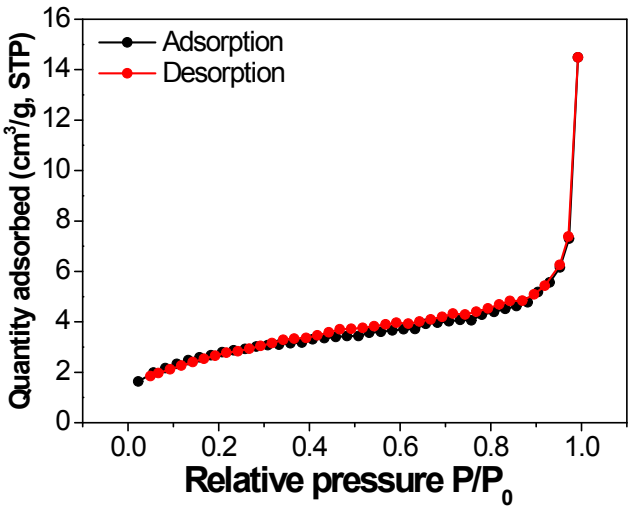

Fig. S6 N_2 adsorption–desorption isotherm at 77 K of micro-YAG:Ce^{3+}

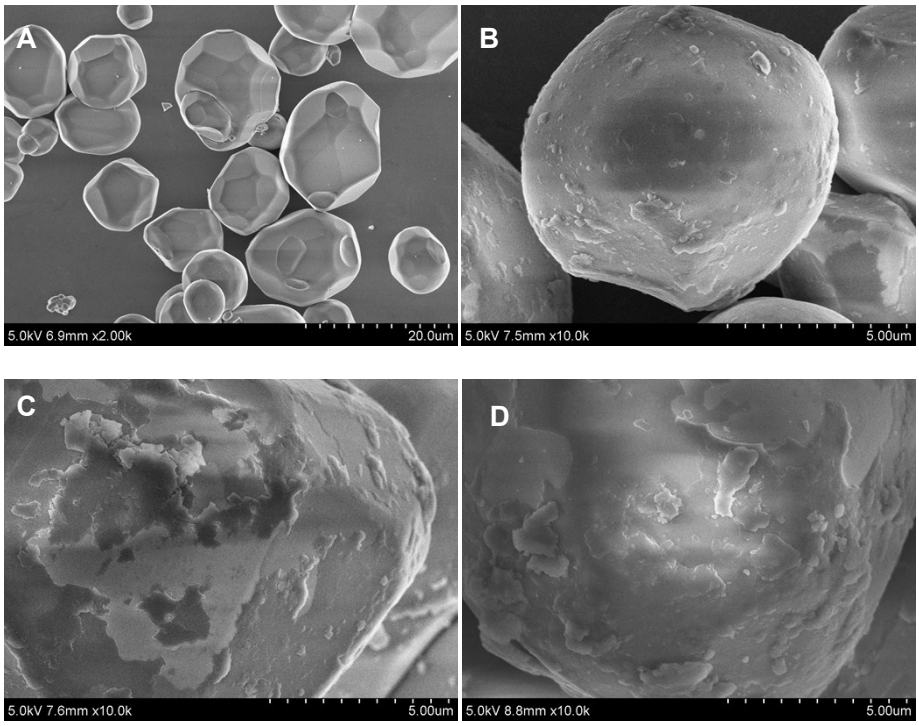

Fig. S7 SEM images of commercial YAG:Ce^{3+} phosphors (A) and the samples after one (B), three (C) and five (D) cycles of surface SiO_2 coating and dye embedding.

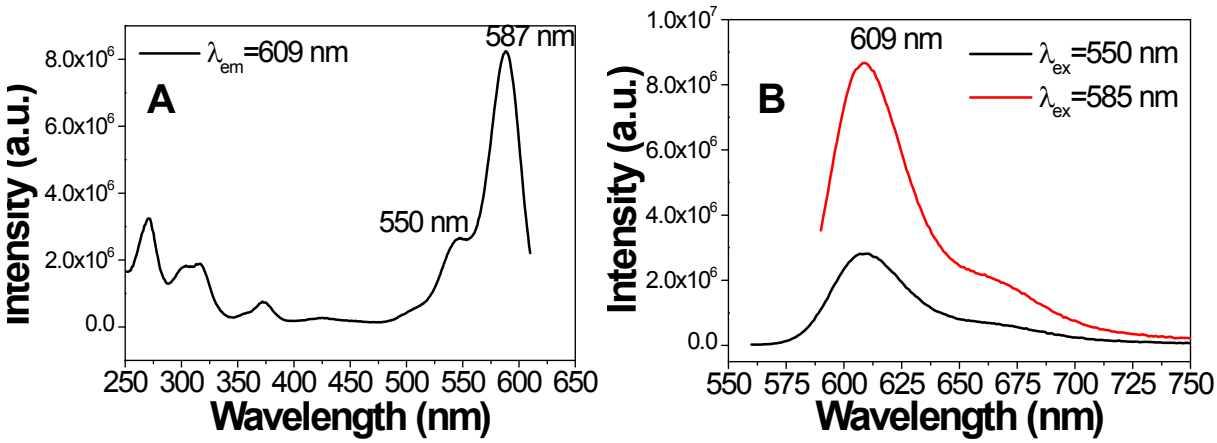

Fig. S8 Excitation (A) and emission (B) spectra of the ethanol dispersions of the dye of ATTO-Rho101-APTS conjugate.

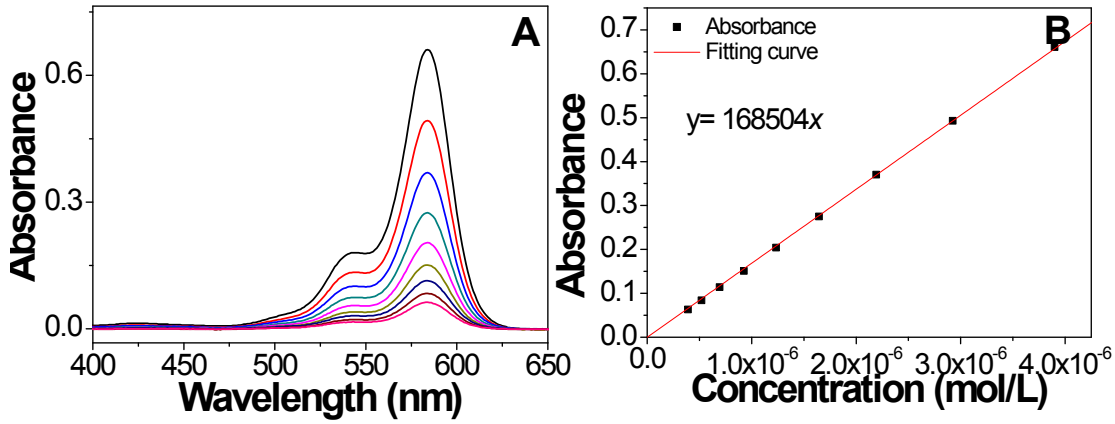

Fig. S9 Absorption spectra of different concentrations of ATTO-Rho101-APTS in ethanol (A) and a fitted calibration curve (B).

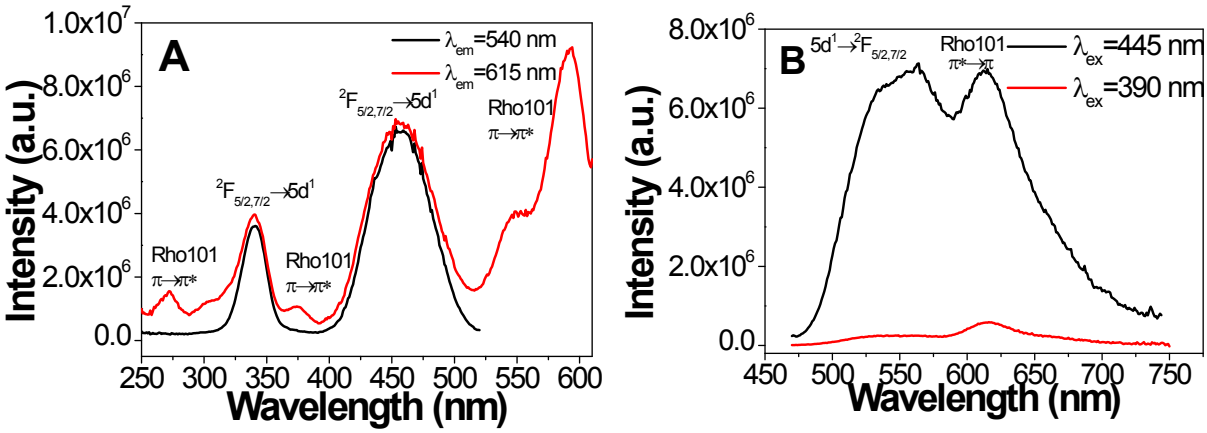

Fig. S10 Excitation (A) and emission (B) spectra of calcined micro-YAG:Ce^{3+} @SiO_2+dye.

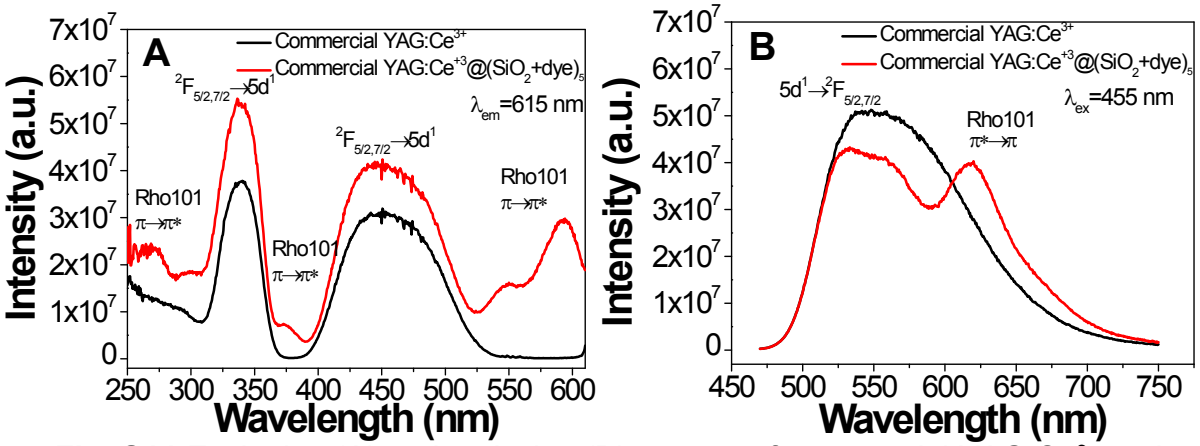

Fig. S11 Excitation (A) and emission (B) spectra of commercial YAG:Ce^{3+} and commercial YAG:Ce^{3+}@(SiO_2+dye)$_5$.

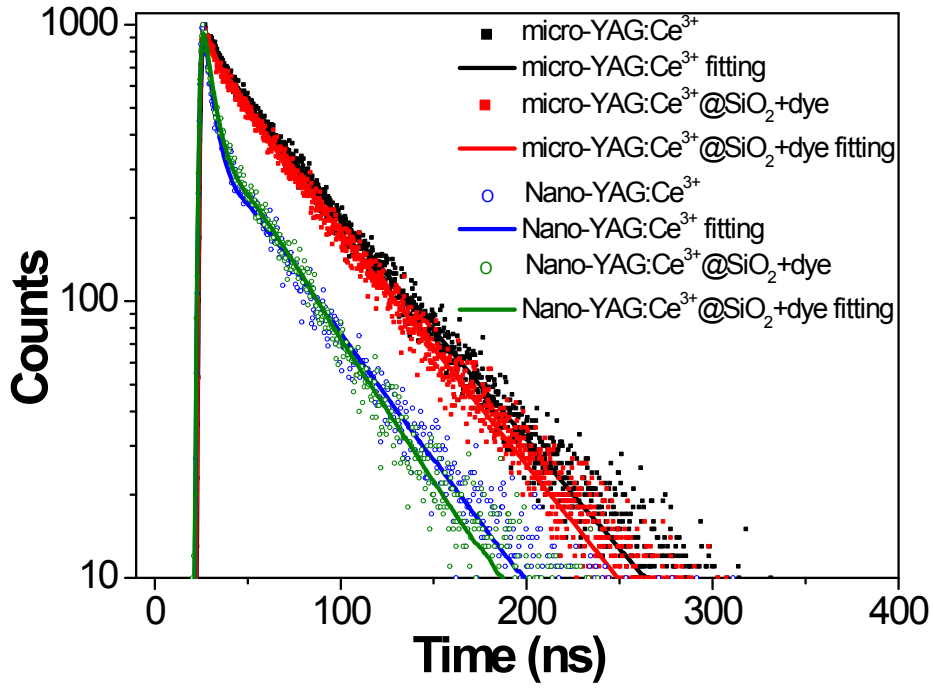

Fig. S12 Fluorescence decays from the lowest-lying $5d^1$ state of Ce^{3+} at λ_{em}=540 nm and their bi-exponential fitting curves of micro-YAG:Ce^{3+} (λ_{ex}=460 nm), micro-YAG:Ce^{3+}@SiO_2+dye (λ_{ex}=460 nm), nano-YAG:Ce^{3+} (λ_{ex}=445 nm) and nano-YAG:Ce^{3+}@SiO_2+dye (λ_{ex}=445 nm).

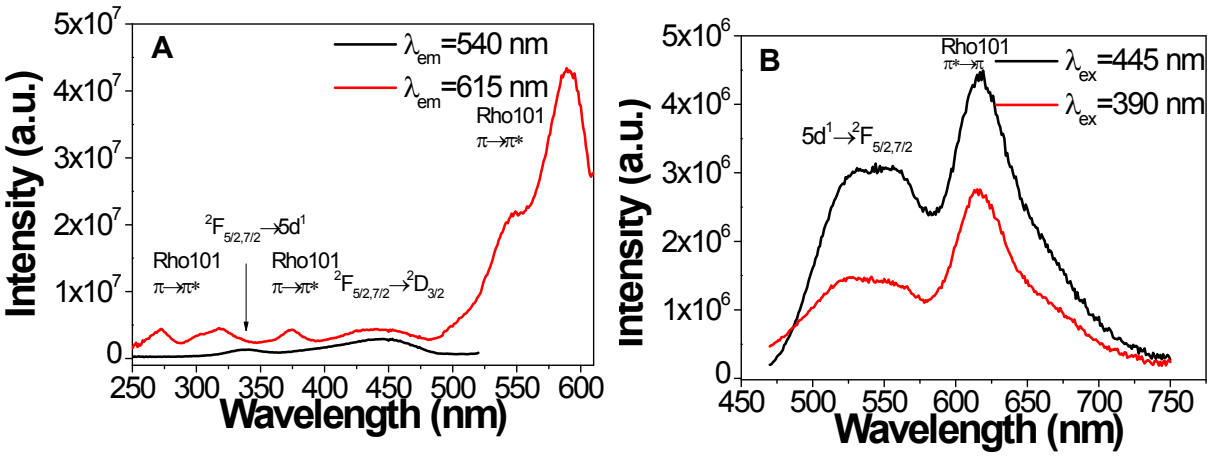

Fig. S13 Excitation (A) and emission (B) spectra of nano-YAG:Ce^{3+}@SiO_2+dye

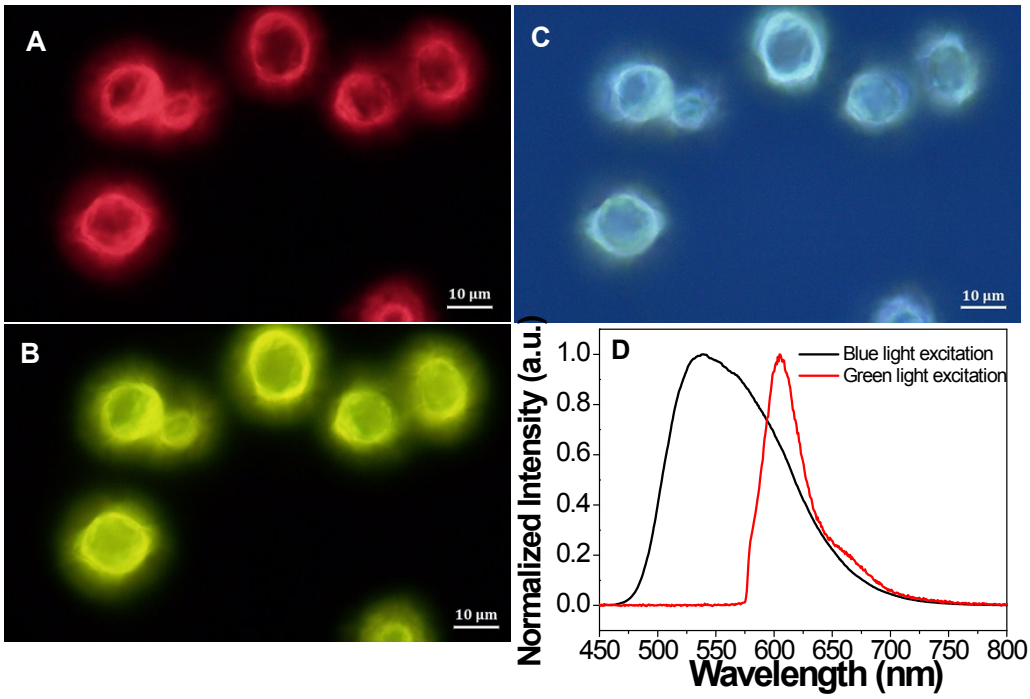

Fig. S14 Fluorescence microscopy images (100×) under blue (A) and green (B) light excitations, and bright field image (C) of highly dispersed commercial YAG:Ce^{3+}@SiO_2+dye as well as *in situ* normalized emission spectra under blue and green light excitations (D).

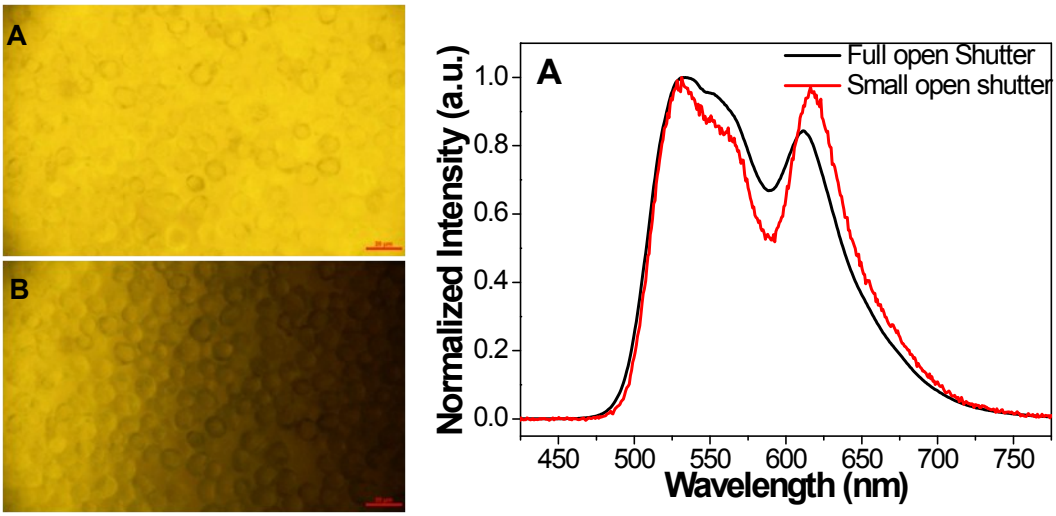

Fig. S15 Fluorescence microscopy images (20×) under blue light excitations with full (A) and small open shutter (B) of accumulated commercialYAG:Ce^{3+}@$(SiO_2$+dye$)_5$ powder layer as well as *in situ* normalized emission spectra (C).

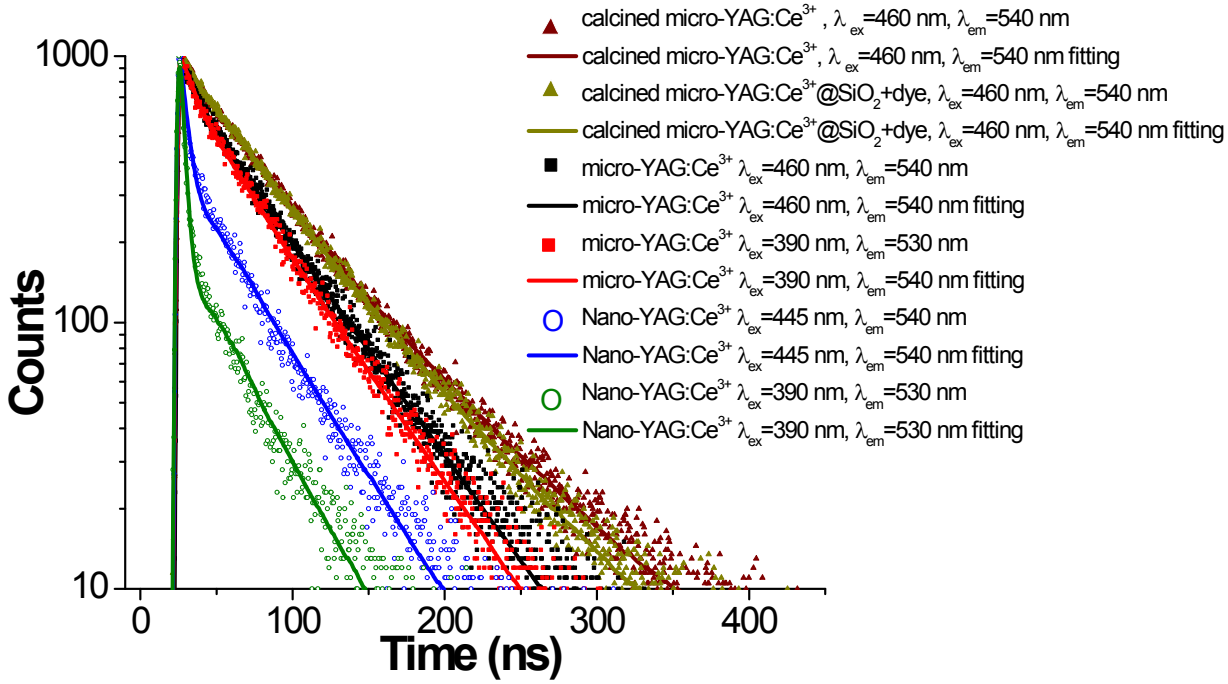

Fig. S16 Fluorescence decays from the lowest $5d^1$ energy level of Ce^{3+} under different wavelength excitations and their bi-exponential fitting curves of micro-YAG:Ce^{3+}, micro-YAG:Ce^{3+}@SiO_2+dye, nano-YAG:Ce^{3+} and nano-YAG:Ce^{3+}@SiO_2+dye.

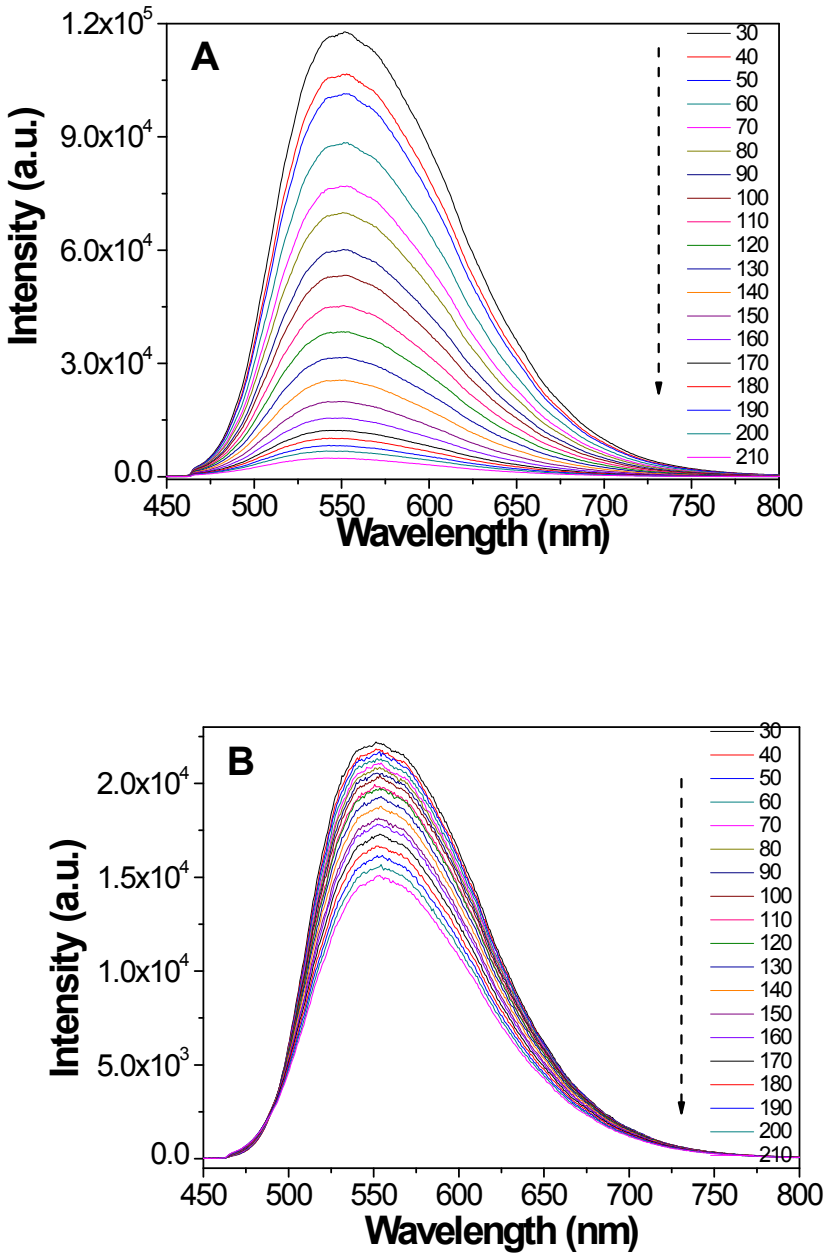

Fig. S17 Temperature dependence of PL spectra under blue light excitation of micro-YAG:Ce^{3+} (A) and micro-YAG:Ce^{3+} after calcinations at 1100^{o}C in N_2/H_2 reduced atmosphere (B) in the range of 30-210 ^{o}C.

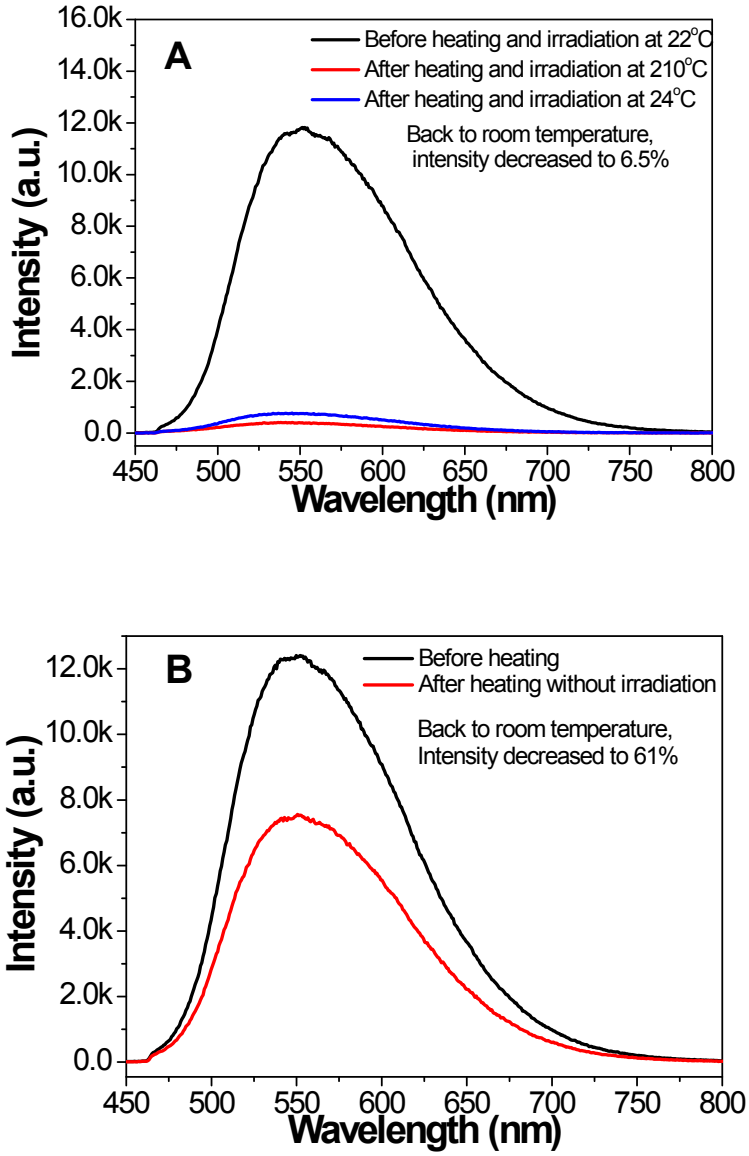

Fig. S18 (A) PL spectra of micro-YAG:Ce^{3+} under blue light excitation at room temperature, 210 °C and then room temperature again after cooling when conducting the temperature dependent PL from 20 to 210 °C; (B) PL spectra of micro-YAG:Ce^{3+} under blue light excitation at room temperature when performing the thermal stability of PL with only heating from 20 to 210 °C but without any irradiation, one spectrum was recorded before the heating ,the other was recorded after cooling to room temperature.

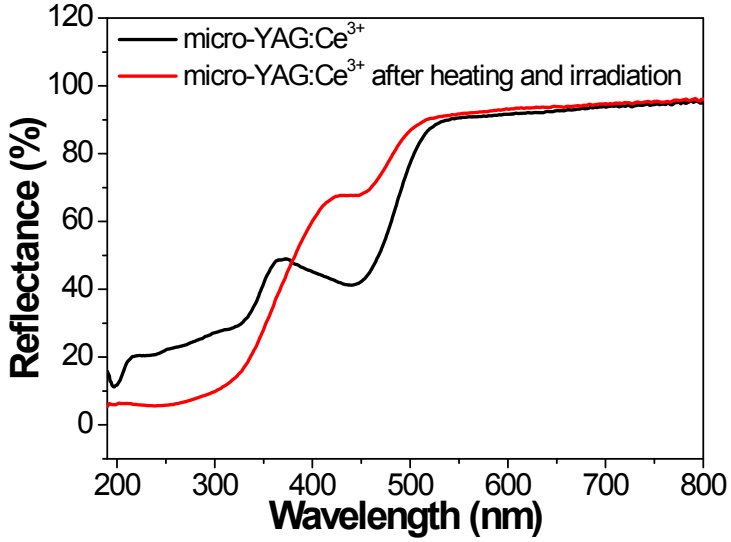

Fig. S19 Diffuse reflection spectra of micro-YAG:Ce^{3+} before and after heating and exciting irradiation at 200^{o}C for 1 h.

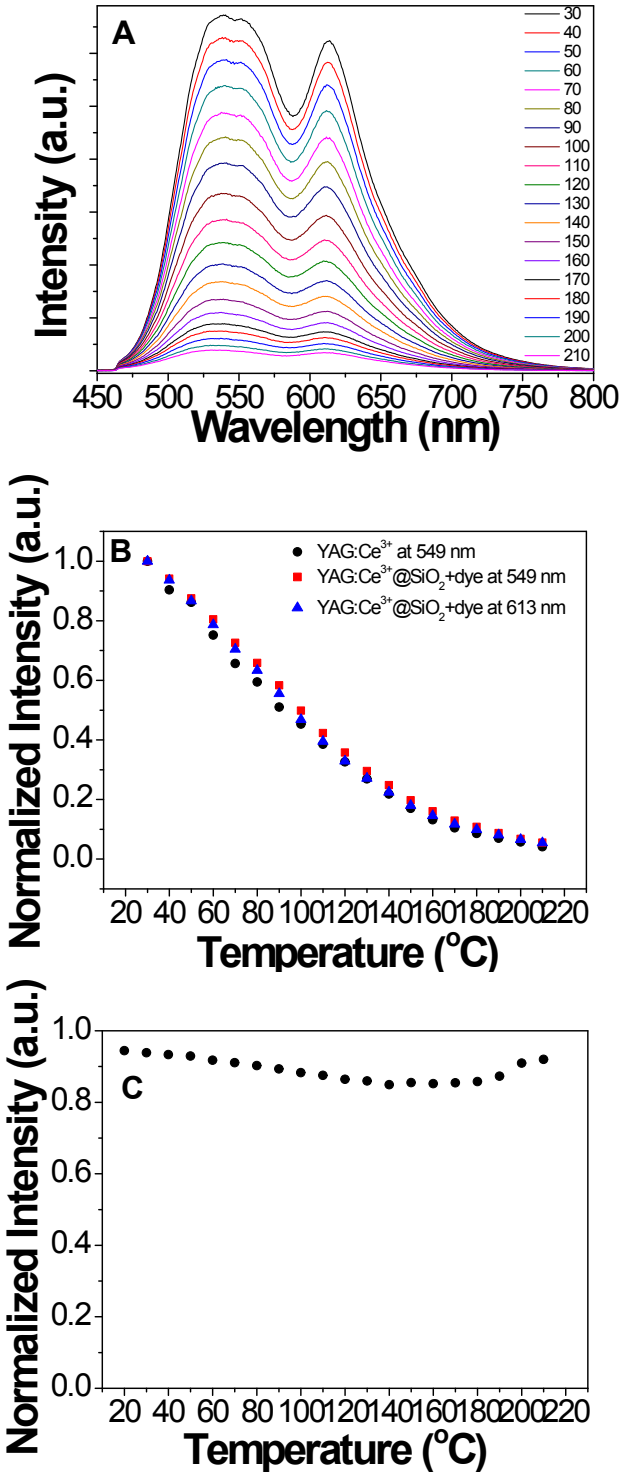

Fig. S20 (A) Temperature dependence of PL spectra of micro-YAG:Ce^{3+}@SiO_2+dye from 30 to 210 °C; (B) Temperature dependence of PL intensity of green emission (~549 nm) of Ce^{3+} and red emission (~613 nm) of micro-YAG:Ce^{3+} and micro-YAG:Ce^{3+}@SiO_2+dye. The PL intensity at different temperatures was normalized to the value at room temperature. (C) The temperature dependence of fluorescence intensity ratio of the red emission (~613 nm) to that of green emission (~549 nm).

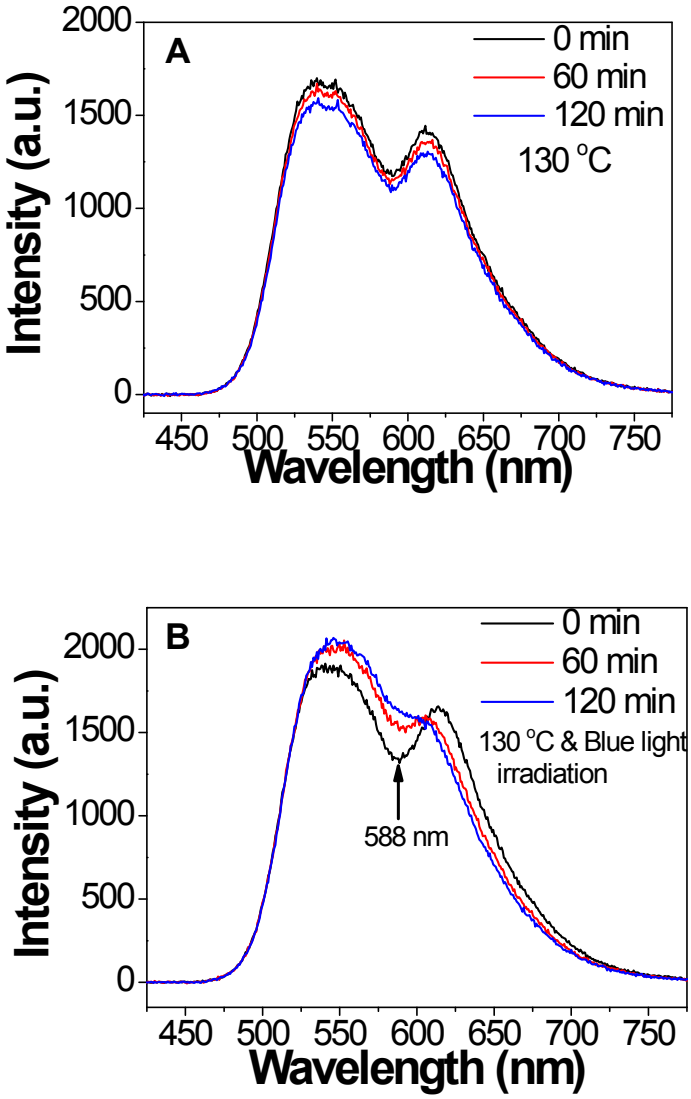

Fig. S21 Thermal stability of PL of commercial YAG:Ce^{3+}@$(SiO_2$+dye$)_5$ at ~130 °C with heating but without irradiation (A) and photo-thermal stability maintaining heating and continuous irradiation meanwhile (B) for 2 h. The spectra were recorded every hour.

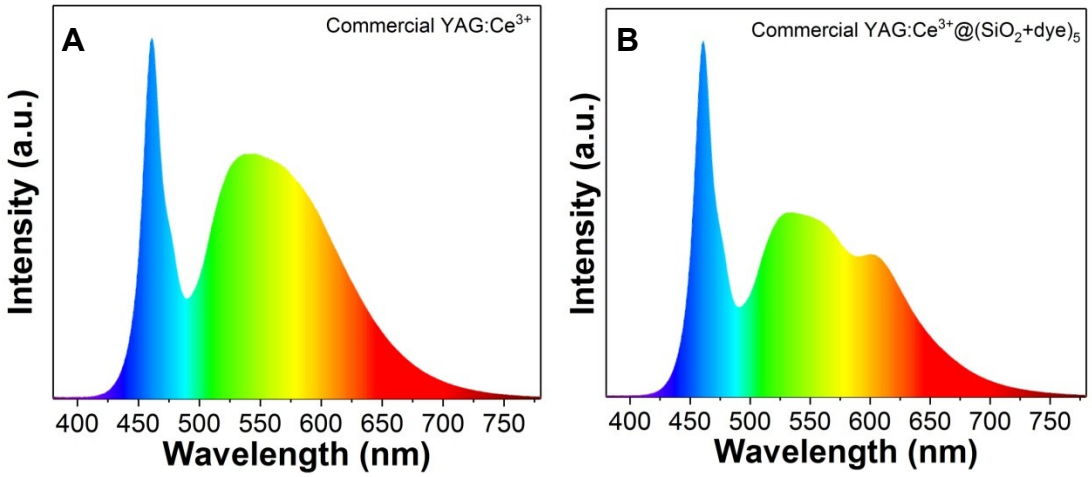

Fig. S22 Electroluminescence (EL) spectra of wLEDs packed with commercial YAG:Ce^{3+} (A) and commercial YAG:Ce^{3+}@$(SiO_2$+dye$)_5$ (B) phosphors.

Table S1 Various performance parameters of wLED packed with calcined micro-YAG:Ce^{3+}, calcined micro-YAG:Ce^{3+}@SiO_2+dye, Commercial YAG:Ce^{3+} and Commercial YAG:Ce^{3+}@$(SiO_2$+dye$)_5$ phosphors and driven with 20 mA current.

Sample	Color rendering index	Color coordinate x, y	Correlated Color temperature, K	Luminous efficacy, lm/W
Calcined micro-YAG:Ce^{3+}	75	0.3299, 0.3857	5597	43
Calcined micro-YAG:Ce^{3+}@ SiO_2+dye	93	0.4117,0.4151	3554	41
Commercial YAG:Ce^{3+}	70	0.3296, 0.3968	5606	221
Commercial YAG:Ce^{3+}@$(SiO_2$+dye$)_5$	79	0.3170, 0.3648	5327	201